Sindh Univ. Res. Jour. (Sci. Ser.) Vol. 50 (004) 561-570 (2018)

http://doi.org/10.26692/sujo/2018.12.0091

SINDH UNIVERSITY RESEARCH JOURNAL (SCIENCE SERIES)

Dynamic structural analysis of connecting rod through adaptive mesh refinement for different materials

I. A. QAZI, A. F. ABBASI, M. S. JAMALI, INTIZAR. A. TUNIO*, M. T. BHATTI**, Q. A. QAZI***

Department. of Mechanical Engineering, Mehran UET Jamshoro, Sindh, Pakistan

Received 19th January 2018 and Revised 7th October 2018

Abstract: In this research dynamic structural behavior of connecting rod made of three different materials has been investigated to choose best suitable and light weighted material for manufacturing of connecting rod without affecting its strength. So in this aspect dynamic structural behavior of connecting rod is analyzed through Finite Element Methods (FEM) by applying two different meshing schemes known as conventional and Adaptive Mesh Refinement (AMR) method. Simulation has been conducted by using ANSYS workbench module. Simulation results have been validated against experimental from literature. From the results of Dynamic structural analysis of connecting rod it is revealed that on the compressive loading maximum stresses occurred in the shank near small end and at its big end. Whereas in case of tensile loading maximum stresses occurred at the mid of inside surface near the smaller end. On the other hand maximum deformation occurs at big end of connecting rod for both compressive and tensile loads. Dynamic structural behavior comparison for connecting rod made of three different materials has also been carried out and it is observed from obtained results that Aluminum alloy experienced highest deformation followed by chromium steel alloy 410. Whereas lowest deformation was found in forged steel material. While comparison of stresses distribution, deformation and weight analysis results for connecting rod made from three different materials, it is concluded that chromium steel alloy 410 connecting rod is lighter in weight as compare to forged steel connecting rod and shown enough strength to sustain the maximum load as compare to aluminum alloy connecting rod. Therefore it is attributed that chromium steel alloy 410 would be better option than the aluminum alloy and forged steel for manufacturing of connecting rod. Furthermore, by comparing the meshing schemes, it is concluded that AMR method provide good results with less computational resources and within less CPU time.

Keywords: Adaptive mesh refinement; Dynamic loading; Connecting rod; Von-Mises stresses, Deformation

1. INTRODUCTION

Connecting rod is a key component of Internal Combustion engine because of its complicated plane motion and intricate shape. During its operation, connecting rod is subjected to time dependent unpredictable tensile as well as compressive loads. Despite of all these working conditions light weighted, high strength and reliable connecting rod is key requirement of design. Now FEA has made its design cycle short and also make it possible to analyze stresses and deformation more accurately.

(Shenoy, 2004a) in this research focused on static and quasi-dynamic structural analysis of connecting rod by using different materials for obtaining optimized results in the premises of its weight and cost. Through his research it is concluded that static analysis results are not sufficient to design connecting rod.

(Adnan. *et al.* 2018) computed stresses and deformation of the connecting rod performed numerical analysis, where it they concluded that in order to improve deformation behavior of the connecting rod the selection of suitable material according to their applications is one the best choice among the several deformation controlling methods.

Shenoy. also compared results of static and quasi-dynamic results and found significant difference in results and suggested that results of quasi-dynamic analysis (using the C-70 Steel material) are the best suitable for optimization of connecting rod.

(Shenoy and Fatemi, 2006) performed FE analysis of connecting rod under static and quasi-static equilibrium to predict axial as well as bending stresses. By following their analysis results it is observed that significant bending stresses are produced in connecting rod, so this should factor be taken into account during design. They also compared the results of static and quasi-static equilibrium simulation and found that significant difference occurs in results of both type of analysis.

(Kaliappan, *et al.*, 2018) In their research they focused that reduced weight of connecting rod efficiently plays role in the operational mechanism and also provides smooth movement of piston and crankshaft inside the IC engine.

(Haider. *et al.*, 2018) in their research they focused that for the improvement of its strength to weight ratiothey performed stress analysis of connecting rod through FEA by considering forged steel, Titanium,

Email: ishfaquealiqazi@gmail.com, fatah.abbasi@faculty.muet.edu.pk, Sharif.jamali@faculty.muet.edu.pk, Intizar_tunio@hotmail.com, trqbhatti@hotmail.com qaziqamarabbas@yahoo.com

*Department of Mechanical Engineering, The Benazir Bhutto Shaheed Technical and Skill Development University, Khairpur (Mirs), Sindh,

**Department. of Mechanical Engineering, Quaid-e-Awam University College of Engineering, Science and Technology, Larkana, Sindh,

***Department. of Mechanical Engineering, Quaid-e-Awam University of Engineering, Science and Technology, Nawabshah, Sindh, Pakistan.

gray cast iron and Aluminum alloy. Their research results indicates that maximum stress occurs at the smaller end of the connecting rod. Form their research it is also found that there are possibilities for reducing of weight of the connecting rod at the shank.

(Fukuda and Eto, 2002) illustrated in their research that the proper design of connecting rod plays more important role to avoid the failure. While designing connecting rod the material's properties, strength economy of material are necessary factors to be focused.

(Saxena and Gupta, 2016) in their research they focused that the inertial forces developed due to reciprocating motion of piston and stresses developed in the form of bending and axial stresses and affect fillet section of the big end and small end of connecting rod. In their research they used CATIA and ANSYS for modeling and simulation respectively. In their research they suggested that these methods can be used for designing of this part with reduced weight and cost without affecting its lifetime. They also illustrated that fatigue crack occur at the transition zone between small end and shank can be analyzed through FEA, which is best suitable method for analysis and design of this part.

(Rabb, 1996) (Griza *et al.*, 2009) described in their research that for the improvements of performance of connecting rod only experimental studies by following the micro structural examination and analysis are not sufficient. But due to complications in analysis through experimental data they suggested that for the enhancement of design strategy of connecting rod and fatigue fracture evaluation, Finite Element Model (FEM) plays an important role.

(Tiwari *et al.*, 2014) conducted static and quasi-dynamic analysis of connecting rod to optimize its fatigue life, reduce weight and compared obtained results of static and quasi-dynamic approaches. Their research concluded that results of static and quasi-dynamic analysis possess significant difference. The designed connecting rod that is 10% lighter in weight than original and 25% less expensive. Material selection for the connecting rod is extremely important stage in production stages of connecting. Proper material selection helps to avoid failure, provide adequate strength and to reduce weight.

(He *et al.*, 2013) (Xu and Yu, 2007) illustrated that improper material selection, defected fabrication, poor designs are the key parameters that lead toward fatigue failure.

(Folgar *et al.*, 1987) developed a fiber FP/Metal matrix composite connecting rod with the aid of FEA, and loads obtained from kinematic analysis. Fatigue was not addressed at the design stage. However, prototypes were fatigue tested. The investigators identified design loads in terms of maximum engine speed, and loads at the crank and piston pin ends. They performed static tests in which the crank end and the piston pin end failed at different loads. Clearly, the two ends were designed to withstand different loads.

(Ilman and Barizy, 2015) identified the reason of failure and to check the fatigue performance of the faulty connecting rod. By using standard failure analysis method and assessment of factors affecting failure including structural design, material type and dynamic loading. The weight optimization of connecting rod is of too very importance factor without compromising the strength, stiffness and fatigue life.

(Gerin, *et al.*, 2017) in their research they investigated the effect of surface finishing and various types of surface defect reduction strategies and concluded that these are the best suitable steps for the improvement of the fatigue strength of the connecting rod. By following experimental results it is also concluded that surface integrity is the influential parameter which affects the fatigue life of connecting rod. Additionally they also concluded that surface defect has significant negative effect on fatigue strength.

(Serag *et al.*, 1989) developed the approximate mathematical formula for predicting weight and material cost for connecting rod. In this research they described that by using geometric programming technique, optimization of connecting rod can be achieved. In their research they focused that during the design of this part with compression stress, bearing pressure at the crank and piston pin ends must be evaluated. Researchers also explained that for obtaining optimized weight of connecting rod and cost function expression must be mentioned in exponential form with geometric parameters.

(Gopinath and Sushma, 2015) conducted research to optimize the weight of connecting rod designed by using the materials i-e Aluminum alloy, Chromium Steel and forged steel. They concluded that mass of optimized connecting rod up to 483g and the optimized geometry of connecting rod is about to 10.38% lighter than of original connecting rod. In the forged steel connecting rod the maximum stresses developed at transition area between pin end, crank end and shank. The applied allowable limit of below 250MPa at the middle of the shank region as the stress value.

(Gu *et al.*, 2005) attributed that strength, stiffness and fatigue behavior are the key properties for selection of material.

(Bansal, 2013) conducted transient FE analysis of connecting rod by using Aluminum alloy. In this research he also illustrated that maximum deformation

occurs at the center of small and big end bearing. It could be concluded through the results of this research that the major connecting rod failures occur due to buckling under critical loads.

2. NUMERICAL SCHEME

2.1 MODELING OF CONNECTING ROD

Connecting rod was modeled in Pro-Engineer software by using engine specification given in **(Table.1).** The 3D model of connecting rod was generated by first developing the two dimensional sketch, then that sketch was extruded. The generated 3D model was further modified to get nearly same connecting rod which is used in selected engine. Modeling accuracies were analyzed by comparing the weight of digitalized 3D model and the actual connecting rod. In Table.1 it is given that actual model of connecting rod is weighing about 439g whereas digitalized three dimensional model has weight of 439.11g; this shows that connecting rod is precisely modeled. In **(Fig.1)** the digitalized model is shown.

Table.1 Shows the Engine specification to which connecting rod belongs.

Crankshaft radius	48.5 mm
Piston diameter	86 mm
Mass of the connecting rod	0.439 kg
Mass of the piston assembly	0.434 kg
Connecting rod length	141 mm
I_{zz} about the center of gravity	0.00144 kg m^2
Distance of C.G. from crank end center	36.4 mm
Maximum gas pressure	37.3 Bar

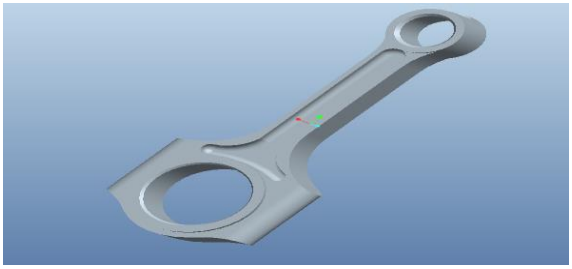


Fig.1 Digitalized three dimensional model of connecting rod

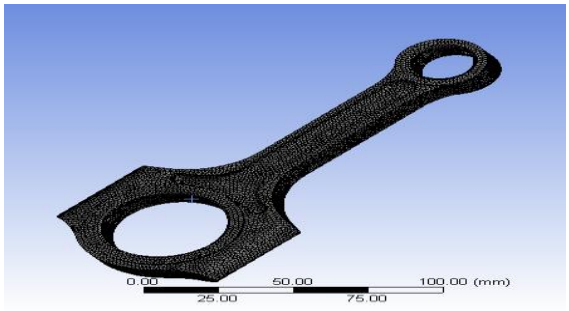


Fig. 2 Meshed model of connecting rod

2.2 Meshing of connecting rod

In present study grid of connecting rod is generated through conventional grid generation technique **(Fig.2)** as well as advanced Adaptive Mesh Refinement (AMR) technique (shown in Fig.16). The AMR technique generates highly refined mesh in the areas of high stress concentration, whereas conventional mesh generation method generate uniform mesh with whole physical domain. AMR technique further enhance solution accuracy by generating high quality mesh with the use of medium computing resources, because it manage number of elements in such a way that region of stress concentration have finest elemental size while other have coarse one. Tetrahedral beam elements were used to generate mesh. Mesh details are given in **(Table. 2. Fig. 2)** shows the meshed model of connecting rod.

Table.2 Connecting rod mesh details

Element Type	Elements	Nodes	Average Orthogonal quality
Tetrahedral	150000	221778	0.85

2.3 Load analysis

In order to predict dynamic structural response of connecting rod throughout the cycle, forces acting on the connecting rod have been calculated by using gas pressure Vs crank angle diagram. Since connecting rod experiences tensile and compressive loads due to inertia of reciprocating components and burnt gas pressure at various instants during cycle, that's why these forces are highly time dependent. In present study both the forces tensile as well as compressive forces have been considered dynamic in nature. Behavior prediction of connecting rod under tensile and compressive forces takes into account. The effect of inertial forces, damping forces as structural non-linearity are also considered. Simulation was conducted for 1.3 second where cycle loads were applied through 13 sub steps at various crankshaft positions. Variation in force acting on the connecting rod against crank angle is shown in **(Fig.3).** From Fig.3 it can be observed that maximum force acting on the connecting rod is at 360o crank angle. From load analysis curve it is observed that connecting rod experiences minimum force at 432o crank angle.

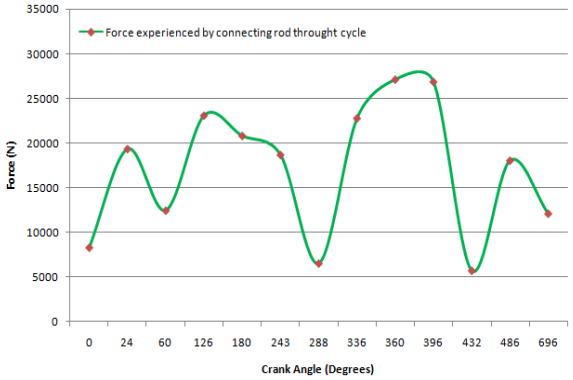


Fig. 3 Force acting on connecting rod throughout the cycle.

2.4 Applied loads and boundary conditions

The constraints as well as loads were applied according the underlying (basic) physics of problem. As the connecting rod is subjected to compression and tension during its operation, therefore it is necessary to conduct its analysis during these both natures of load. During the analysis the tensile as well as compressive loads have been applied over 180o crank contact surface from of connecting rod. The both tensile and compressive loads were distributed uniformly over the crank contact surface. The connecting rod at the piston pin was assumed to be fixed in both of the cases. Therefore restrained load was applied over 180o surface area at the piston pin.

2.5 FEA governing equations

Finite element analysis is a numerical technique which solves complex continuous structural problem by discretizing into small segments known as element. All the elements are connected at one point called node, in between two nodes the element is considered as elastic spring. The whole system behavior is governed by following governing equations.

$$\{F\} = [K]\{u\} \qquad (1)$$

In the equation F denotes applied external load, U represent system behavior and K is the property of material known as stiffness. In case of finite element analysis each element is represented by different equation and finally makes thousand equations. For all cases two variables are known and third one has to be determined therefore equation can be written as.

$$\{u\} = [K]^{-1}\{F\} \qquad (2)$$

In this form above equation looks very easy and can be solved easily but these equations are interconnected at each node and their displacement as well as force transmission affects each other. The given below is case of single spring loaded and distort at both nodes by force f_1 and f_2 distorts by displacement u_1 *and* u_2 then equation can written as:

These equations can be written in matrix form as

$$\begin{pmatrix} k & -k \\ -k & k \end{pmatrix}\begin{pmatrix} u_1 \\ u_2 \end{pmatrix} = \begin{pmatrix} f_1 \\ f_2 \end{pmatrix} \qquad (3)$$

Or

$[k_e]\{u\} = \{F\}$ Whereas $k_e = \begin{pmatrix} k & -k \\ -k & k \end{pmatrix}$

Therefore for three springs in combination then,

$$\begin{pmatrix} k_1 & -k_1 & 0 \\ -k_1 & k_1 + k_2 & -k_2 \\ 0 & -k_2 & k_2 \end{pmatrix}\begin{pmatrix} U_1 \\ U_2 \\ U_3 \end{pmatrix} = \begin{pmatrix} F_1 \\ F_2 \\ F_3 \end{pmatrix}$$

In this way all the equation of discretized domain is connected, solved by Newton Raphson method as follow.

$$X_{n+1} = x_n - \frac{f(x_n)}{f'(x_n)}$$

2.6 VALIDATION OF FEA MODEL

In this section results of FEA are validated with published work in order to ensure that modeled finite element setup is reliable, so that same procedure can be used for further system improvement. In order to validate FEA model Von-Mises stresses has been calculated along the half way in shank region. These stress values are obtained by applying maximum tensile and compressive force experienced by connecting rod during cycle. Those obtained stress values at these points are compared and shown in **(Table.3a)** and **(Table.3b).** By comparing experimental values of Von-Mises stresses with obtained FEA results (shown in **(Fig. 4 and Fig. 5),** it is concluded that modeled FE setup shows good agreement with experimental results for both compressive and tensile loading. While calculating error between Experimental results and simulation results it is observed that difference is minimum at two points whereas its value increase up to 2.7% for single point at the center of shank surface along the half way in shank region. Similar trend of increased difference was also observed for compressive.

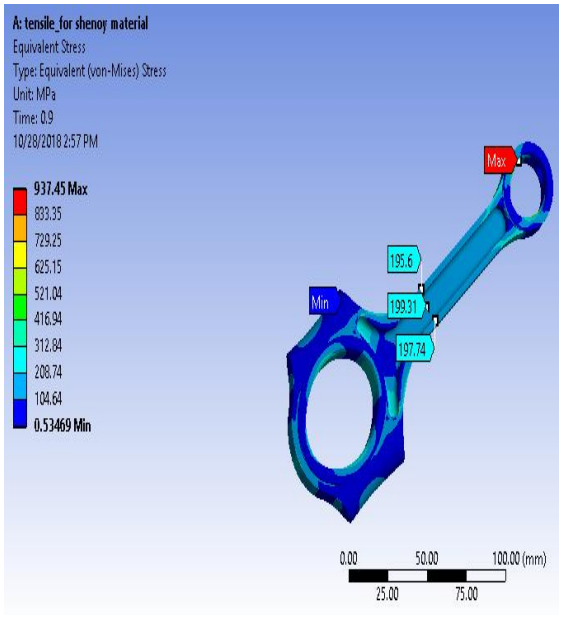


Fig.4 FEA simulation results for tensile

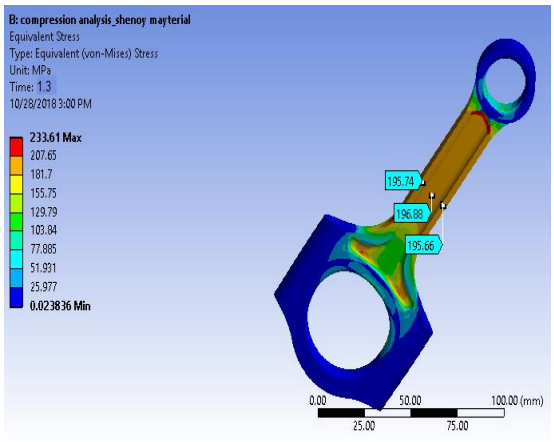


Fig.5 FEA simulation results for compressive

Table: 3a) Validations of finite element model with published research work (Shenoy, 2004b)

	Maximum Tensile Load (26.841KN)		
Points on shank	**Experimental Results**	**Simulated Results**	**Diff (%)**
	Von Mises	**Von Mises**	
1	196.5	195.6	0.46
2	205	199.3	2.87
3	196.5	197.7	-0.63

Table: 3(b) Validations of finite element model with published research work (Shenoy, 2004b)

	Maximum Compressive Load (26.841KN)		
Points on shank	**Experimental Results**	**Experimental Results**	**Experimental Results**
	Von Mises	**Von Mises**	**Von Mises**
1	197.1	197.1	197.1
2	202	202	202
3	197.1	197.1	197.1

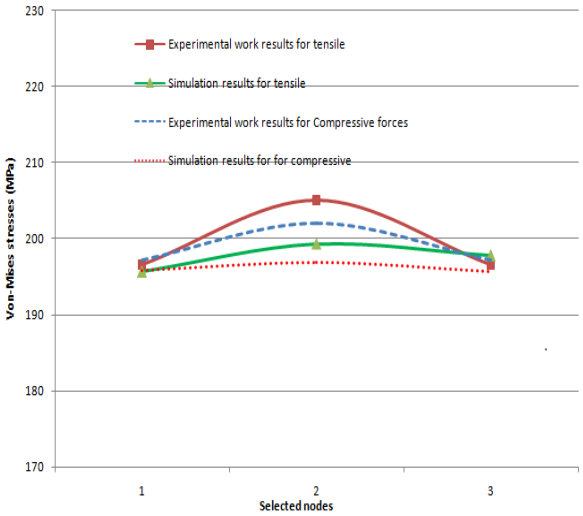


Fig. 6 comparison of FEA simulation results with published experimental work (Shenoy, 2004b)

3. RESULTS AND DISCUSSION

3.1 Stress analysis of connecting rod through conventional FEM

In this section results for stress analysis of connecting are present for both tensile and compressive loads. Stress results are presented in terms of Von-Mises stresses and Shear stresses produced in the connecting rod. In **(Fig.7)** the Von-Mises stress distribution due to compressive load is present. In Fig.7 from the values of Von-Mises stress it was observed that maximum stress produced in connecting rod is lower than material yield strength, hence it can be concluded that the design of connecting rod is safe keeping in view stress results. From Fig. 7 it was also observed that maximum Von-Mises stress occurs in shank area near the smaller and bigger end of the connecting rod. From Von-Mises stress distribution within the connecting rod due compressive load it is analyzed that very low stresses are produced in both the bigger and smaller end of connecting rod. In Fig.8 the results of shear stress distribution within connecting rod due to compressive load are presented. While observing shear stress distribution in connecting rod due to compressive load, it is concluded that shear stress distribution is completely following Von-Mises stress distribution. On the other hand maximum value of Von-Mises stress is much higher than maximum shear stress value.

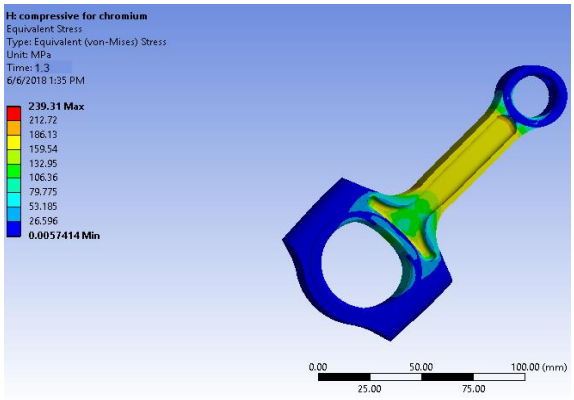


Fig. 7 Von-Mises stress distribution due to compression

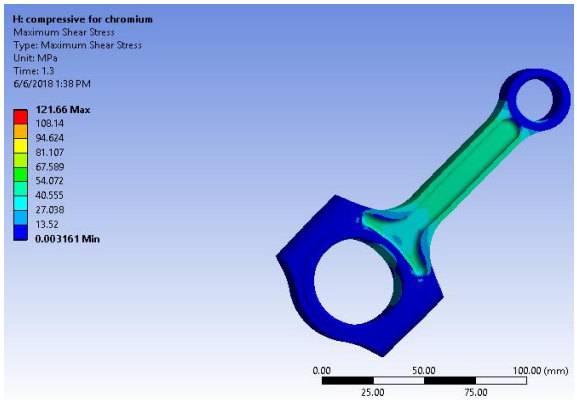


Fig. 8 Shear stress distribution due to compression

The results of stress distribution within connecting rod due to tensile forces are present in Fig.9 and Fig.10. While observing Von-Mises stress distribution within connecting rod due to tensile load, it is observed that maximum stress occur at mid of inner side of smaller end. From **(Fig.9)** it could be concluded that very small amount of stress produced at the bigger end of connecting rod. In **(Fig.10)** results of shear stress distribution within connecting rod due to tensile forces are present. After careful observation of shear stress distribution within connecting rod it is concluded that shear stress distribution follows same trend of von-Mises stress distribution for tensile loading. After analyzing stress distribution within connecting rod due tensile and compressive loading, it is clear that stress distribution is very much opposite for both type stresses. From above mentioned observations it is also found that very small amount stresses produced due compressive in comparison of tensile loading.

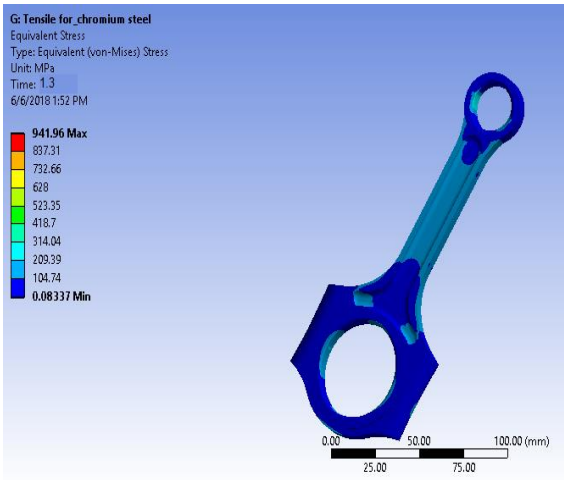


Fig.9 Von-Mises stress distribution under tensile loading

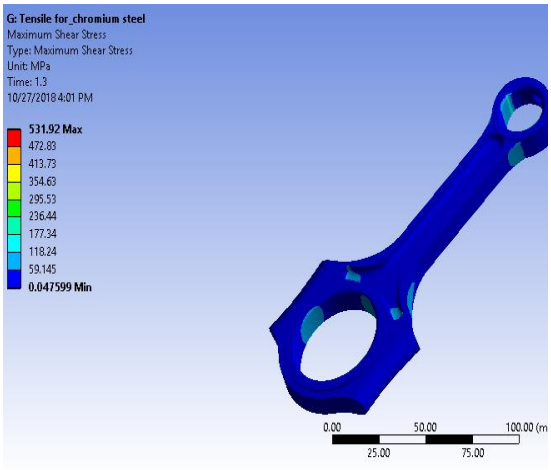


Fig.10 Shear stress distribution under tensile loading

In **(Fig.11)** the variation of Von-Mises stresses against crank angle has been presented and compared for tensile as well as compressive forces. From **(Fig.11)** it is observed that maximum von-Mises stresses would be produced at 336ºwithin connecting rod crank angle whereas minimum stresses would occur at 432º crank angle in case of tensile loading. While observing the stress variation during cycle under compressive loading, almost similar trend in stress variation was observed.

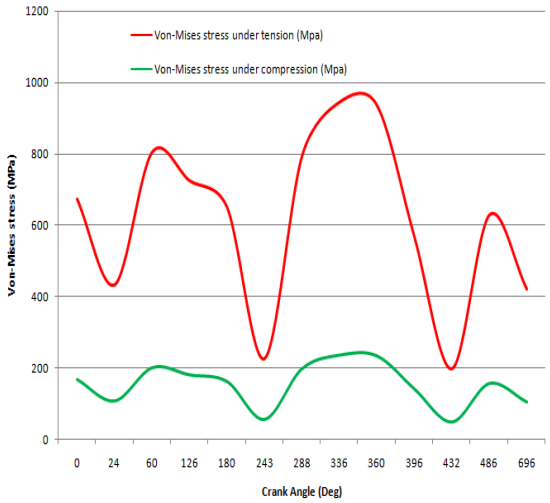


Fig.11 Von-Mises stress variation during cycle for tensile and compressive loads

In **(Fig.12)** the variation of shear stresses against crank angle has been presented and compared for tensile as well as compressive forces. From Fig.12 it is observed that maximum shear stress would be produced at 336º within connecting rod crank angle, whereas minimum stresses would occur at 432º crank angle in case of tensile loading. While observing the stress variation during cycle under compressive loading, almost similar trend in stress variation was observed

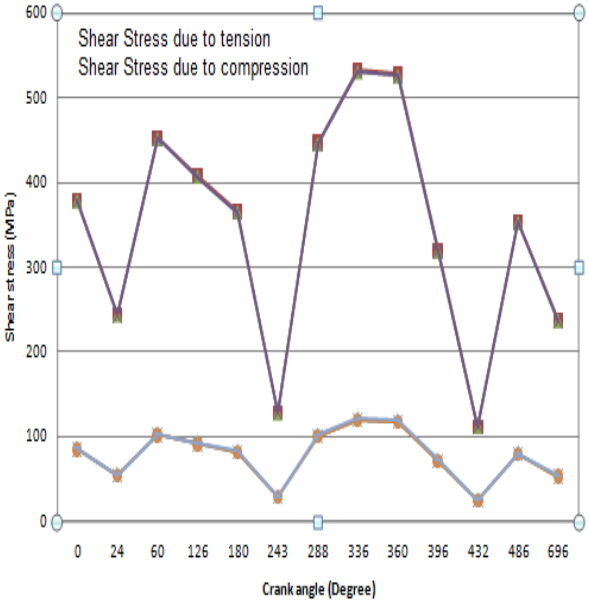


Fig.12 Shear stress distribution during cycle for Tensile and compressive loads for three different materials.

3.2 Deformation Analysis of Connecting Rod Through Conventional FEM

Deformation produced within connecting rod due tensile and compressive loading are presented. In Fig. 13 deformation produced due tensile loading is presented. From **(Fig.13)** it is observed that maximum deformation is produced in bigger end cap. While careful observation of deformation produced in connecting rod reveal that deformation is minimum at smaller end and it increase along the connecting rod length. From **(Fig.14)** it was observed that deformation produced in connecting rod due compressive forces follows almost same pattern of deformation due tensile loading but maximum deformation occurs at crank end, on the in case of tensile loading maximum deformation occurs only crank end cape. Comparing the deformation produced due compressive and tensile loading it is observed that deformation value in case of tensile loading is much higher than in compression

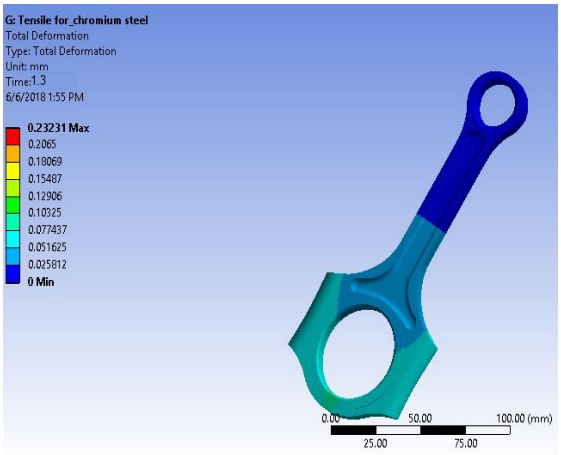


Fig.13 Deformation produced in connecting rod due to tension

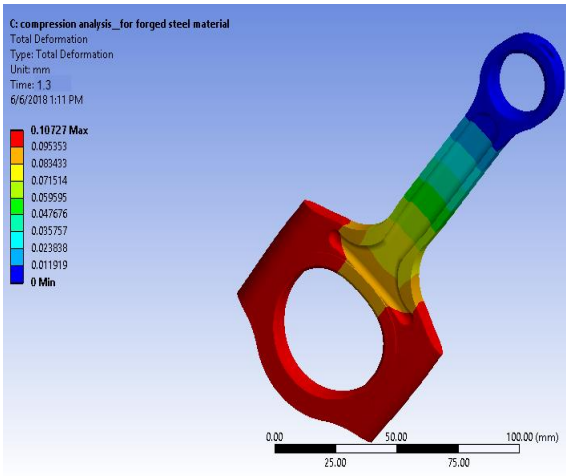


Fig.14 Deformation produced in connecting rod due to compression

In **(Fig.15)** the variation of deformation against crank angle has been presented and compared for tensile as well as compressive forces. From Fig.15 it was observed that maximum deformation would be produced at 336º within connecting rod crank angle whereas minimum deformation would occur at 432º crank angle in case of tensile loading. While observing the deformation variation during cycle under compressive loading, almost similar trend in deformation variation was observed.

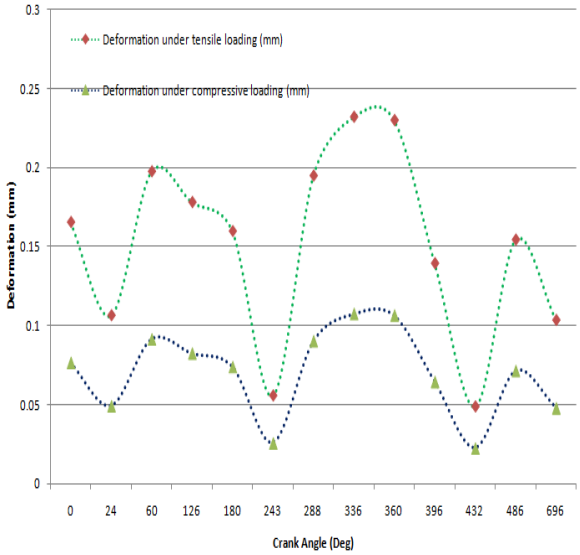


Fig.15 Deformation variation during cycle for tensile and compressive loads

3.3 Dynamic Structural behavior prediction of connecting rod made from different materials

In this section dynamic structural behavior analysis results for connecting rod made of three different materials of are present. Comparison is made on basis of connecting rod deformation and its weight. So weight calculation of connecting rod when it is made up of different material is possible by considering (focusing) mechanical properties of these materials. The mechanical properties of the selected materials like forged steel, Aluminum Alloy and Chromium alloy steel 410 are given in Table.4. Here **(Fig.16)** shows the weight comparison graph for connecting rod when it is made from different materials. From plotted graph in Fig.16 it is found that Aluminum alloy has lowest weight of 151.7g followed by Chromium steel alloy weighing 432.5g, and forged steel connecting rod has highest weight of 440.9g. While observing deformation graph in **(Fig.17)** it has been found that maximum deformation occurs at 360º during cycle under compression loading, whereas minimum deformation occurs at 243º and 432º crank angle. From Fig.17 it has been observed that connecting rod made from Aluminum alloy experiences highest deformation followed by chromium and forged steel. From Fig.17 it is also concluded that three different materials used for manufacturing of connecting rod has almost similar deformation behavior under dynamic compression

loading. Whereas in **(Fig.18)** it is described that how much deformation is going to be produced within connecting rod when it is analyzed under tensile loading. After careful observation of deformation behavior within the connecting rod due to tensile loading, it is concluded that its deformation behavior due to tensile loading is very similar to the connecting rod deformation behavior under compression loading.

Table: 4 Mechanical properties of selected materials

Name of Materials	Young's Modulus (E)	Poisson's ratio	Density
Forged steel	200 GPa	0.3	7850 Kg/m^3
Aluminum Alloy	70 GPa	0.33	2700 Kg/m^3
Chromium alloy steel 410	200 GPa	0.3	7850 Kg/m^3

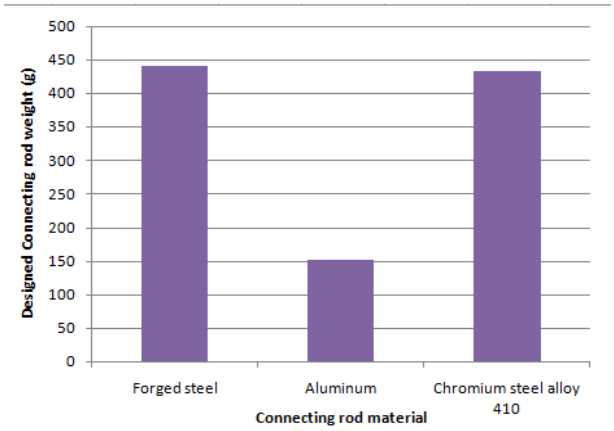


Fig. 16 Connecting rod weight comparison for different materials

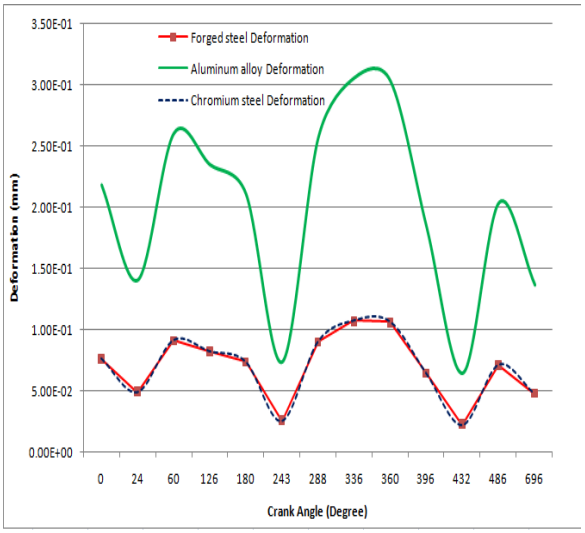


Fig. 17 Connecting rod deformation comparison for different materials under compressive load

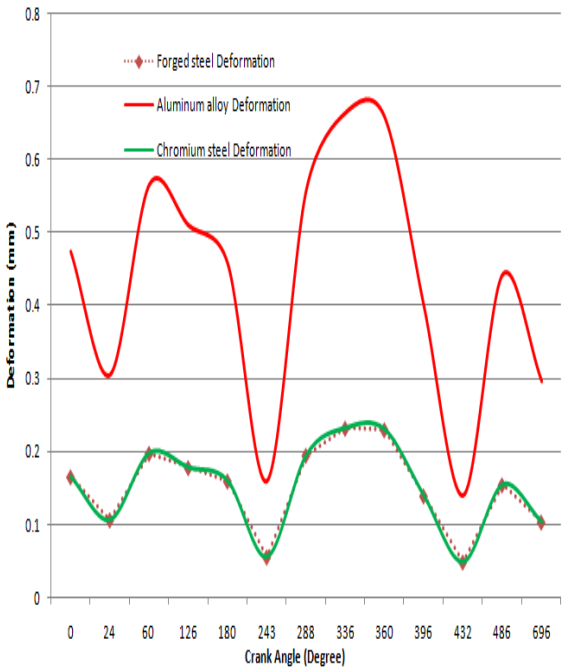


Fig. 18 Connecting rod deformation comparison for different materials under tensile load

3.4 Dynamic structural behavior prediction of connecting rod through AMR.

In this section results of dynamic structural behavior of connecting through AMR method are present and compared with results of conventional mesh method. As the results obtained from AMR method are present in Fig.19. In Fig.19 stress distribution within connecting rod is shown and stress concentration area near small end is presented in zoomed view. While observing Fig.19 it is observed that maximum value Von-Mises stresses obtained though AMR method is much higher as compared to obtained value through conventional method. From Fig.19 it is also noticed that mesh was only refined in high stress area. During analysis simulation time was also noticed for two mentioned methods named as AMR and conventional mesh method. It is found that conventional mesh method require CPU time approximately twice of AMR method. At the same time number of elements used by conventional meshing method is 150556 while meshing carried through AMR only contains 34133 elements at highly concentrated area. In Fig.20 results of Von-Mises stress variation are present during the cycle for two different meshing methods. From Fig.20 it has been also noticed that stress values obtained through AMR meshing method are higher than values obtained from conventional meshing method during whole cycle

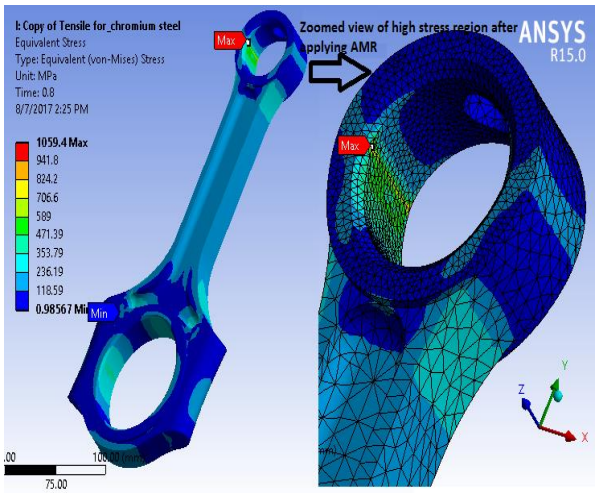


Fig. 19 Von-Mises stress distribution connecting rod through AMR meshing technique

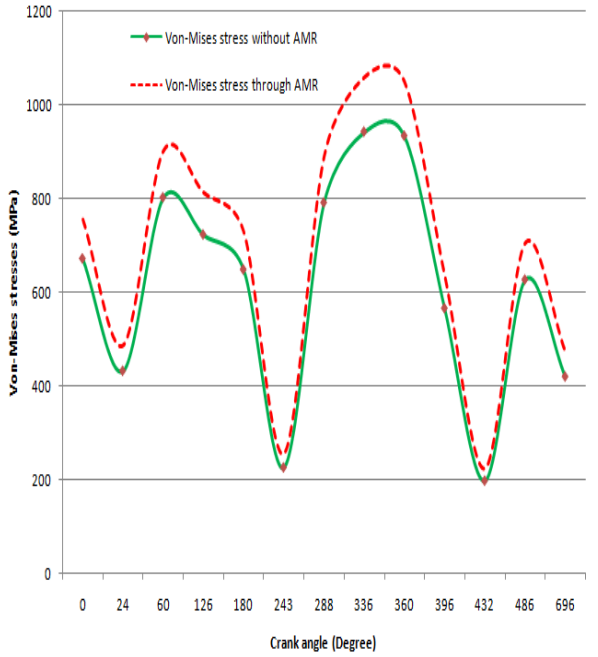


Fig. 20 Comparison of Von-Mises stress variation within connecting rod during cycle through two different meshing methods.

4. CONCLUSION

The dynamic structural analysis of connecting rod revealed the following conclusion

- From the stress distribution within connecting rod, it is found that maximum stresses occur in the shank near smaller and bigger end of the connecting rod in case of compressive loading.
- Stress distribution within connecting rod under tensile load results revealed that maximum stresses occur at the mid of inside surface near the smaller end of connecting rod.
- From deformation analysis results it is found that maximum deformation occur at big end of connecting rod for both compressive and tensile loads.
- From dynamic structural behavior comparison of connecting rod for three different materials it is found that highest deformation is produced in aluminum alloy followed by chromium steel alloy 410 whereas lowest deformation was experienced by forged steel.
- On the basis of stresses distribution, deformation and weight analysis for three different materials it is concluded chromium steel alloy 410 connecting rod (432.5g) has lighter weight and showed enough strength to sustain load.
- On the basis of above discussed criteria chromium steel alloy 410 would better option than aluminum alloy and forged steel.
- On the basis of comparison made between conventional and AMR mesh methods it is concluded that AMR method provide accurate results with less computational resources and within half simulation time.
- On the basis of the results extracted during the conventional and AMR meshing methods, it is concluded that Adaptive mesh refinement (AMR) is such a version of FEA analysis tool (software) which provides analysis solutions at high concentrated region of any part.

REFERENCES:

Adnan A. H., A. Kumar, A. Chowdhury, M. Khan, and P. Suresh, (2018) Design and Structural Analysis of Connecting Rod, International Research Journal of Engineering and Technology (IRJET), Vol.05 Issue: 05.

Bansal, R. (2013) Dynamic Simulation of a Connecting Rod Made of Aluminium Alloy Using Finite Element Analysis Approach. *IOSR Journal of Mechanical and Civil Engineering*, 5**,** 01-05.

Fukuda, S. and H. Eto, (2002) Development of Fracture Splitting Connecting Rod. *JSAE review*, 23**,** 101-104.

Gopinath, D. and C. V. Sushma, (2015) Design and Optimization of Four Wheeler Connecting Rod Using Finite Element Analysis. *Materials Today: Proceedings*, 2**,** 2291-2299.

Griza, S., F.Bertoni, G. Zanon, A. Reguly, and T.Strohaecker, (2009) Fatigue in Engine Connecting Rod Bolt Due to Forming Laps. *Engineering Failure Analysis*, 16**,** 1542-1548.

Gu, Z., S. Yang, S. Ku, Y. Zhao, and X. Dai, (2005) Fracture Splitting Technology of Automobile Engine Connecting Rod. *The International Journal of Advanced Manufacturing Technology*, 25**,** 883-887.

Gerin, B., E. Pessard, F. Morel, and C. Verdu, (2017). Influence of surface integrity on the fatigue behaviour of a hot-forged and shot-peened C70 steel component. Materials Science and Engineering: A, 686, 121-133.

Haider, A. A., A. Kumar, A. Chowdhury, M. Khan, and P. Suresh, (2018). Design and Structural Analysis of Connecting Rod.

He, B.Y., J. Sun, S.Z. Chen,. and R. Nie, (2013) Crack Analysis on the Toothed Mating Surfaces of a Diesel Engine Connecting Rod. *Engineering Failure Analysis,* 34**,** 443-450.

Ilman, M. and R. Barizy, (2015) Failure Analysis and Fatigue Performance Evaluation of a Failed Connecting Rod of Reciprocating Air Compressor. *Engineering Failure Analysis*, 56**,** 142-149.

Kaliappan, S., R. Raam, B. Charan, S. Asswin, M. Ibrahim, S M. Mothilal, M.D. Rajkama, (2018) Modal And Kinematic Analysis Of A Connecting Rod For Different Materials in International Journal of Pure and Applied Mathematics. Volume 119 No., 14599-14608, ISSN:1314-3395.

Rabb, R. (1996) Fatigue Failure of a Connecting Rod. *Engineering Failure Analysis,* 3**,** 13-28.

Saxena and Gupta (2016) A Review on Different Methods of Failures of Connecting Rod in Internal Combustion Engine. *International Journal of Inovative Engineering Resarch,* 6.

Serag, S., L. Sevien, G. Sheha, and I. El-Beshtawi, (1989) Optimal Design of the Connecting-Rod. *Modelling, Simulation and Control, B,* 24**,** 49-63.

Shenoy, P. S. (2004a). *Dynamic Load Analysis and Optimization of Connecting Rod.* University of Toledo.

Shenoy, P. S. and A. Fatemi, (2006) Dynamic Analysis of Loads and Stresses in Connecting Rods. *Proceedings of the Institution of Mechanical Engineers, Part C: Journal of Mechanical Engineering Science,* 220**,** 615-624.

Tiwari, A.. J. K. Tiwari, and S. K. Chandrakar, (2014) Fatigue Analysis of Connecting Rod Using Finite Element Analysis to Explore Weight and Cost Reduction Opportunities for a Production of Forged Steel Connecting Rod. *International Journal of Advanced Mechanical Engineering,* 4**,** 782-802.

Xu, X. L. and Z. W. Yu, (2007) Failure Analysis of a Diesel Engine Connecting Rod. *Journal of Failure Analysis and Prevention,* 7**,** 316-320.